Surfing Multiple Conformation-Property Landscapes via Machine Learning: Designing Single-Ion Magnetic Anisotropy.

Alessandro Lunghi* and Stefano Sanvito

School of Physics, AMBER and CRANN Institute, Trinity College, Dublin 2, Ireland

E-mail: lunghia@tcd.ie

Abstract

Computational statistical disciplines, such as machine learning, are leading to a paradigm shift in the way we conceive the design of new compounds, offering a way to directly design the best compound for specific applications. This approach, known as reverse engineering, requires the construction of models able to efficiently predict continuous structure-property maps. Here we show that machine-learning offers such a possibility by designing a model that predicts both the energy and magnetic properties as function of the molecular structure of single-ion magnet. This model is then used to explore the molecular conformational landscapes in search of structures that maximise magnetic anisotropy. We find that a 5% change in one of the coordination angles leads to a $\sim$50% increase in the anisotropy. This approach can be applied to any structure-property relation and paves the way for a machine-learning-driven optimization of chemical compounds.

Introduction

The design of new materials with specific target properties is the ultimate goal of reverse materials engineering. This approach requires the construction of a range of maps between the chemical structure $\{r_i, Z_i\}$ and the properties of interest $P(\{r_i, Z_i\})$.[1] In this framework, the design process corresponds to the optimization of a global target function, χ, that weighs different properties,

$$\max_{\{r_i,Z_i\}} \chi = \sum_l \gamma_l P(\{r_i, Z_i\}) \,, \tag{1}$$

where $\{r_i, Z_i\}$ contains the position and atomic number of the atoms forming the material and the weights, γ_l, set the relative importance of the single properties, P_l.

While in principle quantum mechanical methods could be used for such a task, their computational overheads render them impractical. Machine-learning-based models, with their ability to reproduce quantum mechanical results at a negligible computational cost, are the perfect tool to construct reverse engineering and generative approaches.[2–5] In this work we develop an efficient framework to build and explore general properties-structure maps and apply it to a topical case of technological importance, namely magnetic materials.

Magnetism is an exotic phenomenon that emerges from a very delicate balance between the electronic and structural properties of chemical compounds. Magnetic compounds form a paradigmatic materials class containing rare members with large technological impact. The working principle of hard magnets is based on the presence of a large axial magnetic anisotropy that stabilises the magnetic moment against thermal fluctuations. This picture can be formally explained with the spin Hamiltonian

$$\hat{H}_S = D\hat{S}_z^2 \,, \tag{2}$$

where $\hat{S}_z$ is the z component of the spin operator and a negative D parameter corresponds to an axial anisotropy. When the magnetic anisotropy is not large enough to overcome thermal

fluctuations or when a magnet is perturbed by external stimuli, demagnetization processes take place. Spin relaxation in non-metallic materials is ultimately due to the interaction between the magnetic and lattice degrees of freedom, namely the spin-phonon coupling. This interaction manifests itself through the dependence of the magnetic anisotropy tensor $\mathbf{D}(r_i)$ on the atomic positions r_i. In general $\mathbf{D}(r_i)$ is interpreted in terms of a Taylor expansion around the equilibrium molecular geometry $r_{i,0}$:

$$\mathbf{D}(r_i - r_{i,0}) = \mathbf{D} + \sum_i \left(\frac{\partial \mathbf{D}}{\partial r_i}\right)_0 (r_i - r_{i,0}) + ... \tag{3}$$

The understanding of the microscopic processes leading to spin-phonon coupling and demagnetization is of interest for several applications such as heat-assisted magnetic recording,[6] ultra-fast demagnetization,[7] magnetostriction,[8] spintronics,[9] molecular magnetism[10,11] and quantum computing based on electronic spins.[12,13]

The design of magnetic materials is a prototypical example where multiple features must be optimized at the same time to reach optimal efficiency. Eq. (3) suggests that making high-temperature hard-magnets requires: i) the maximization of the axial magnetic anisotropy $|D|$, ii) the minimization of its derivatives (the spin-phonon coupling coefficients), and iii) little thermally populated molecular motions $(r_i - r_{i,0})$. This effectively corresponds to the design of $\mathbf{D}(r_i)$ having a maxima in correspondence of the equilibrium geometry and a very stiff material.[10]

We have applied our method to molecular magnets, which appear as the ideal materials class for a systematic design strategy. These compounds represent the ultimately small building blocks of magnetic recording media.[14] At the same time the combination of density functional theory (DFT) and post Hartree-Fock methods is ideal for predicting their structural and magnetic properties.[15] Finally, and most importantly, the extensive synthetic versatility of such coordination compounds allows one to fine tune the structure, so that design is practically possible. In particular, we here restrict the challenge of optimizing Eq.

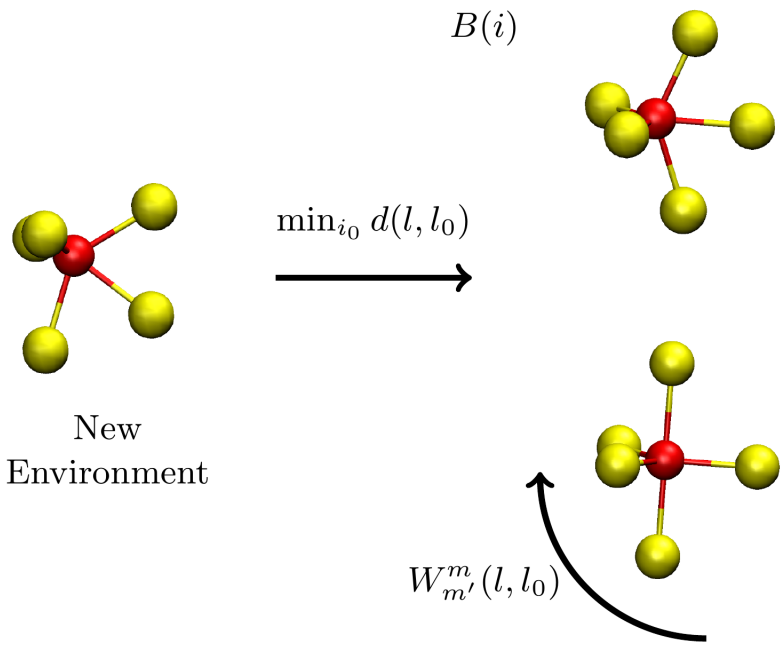

Figure 1: **Scheme for Structural Recognition and Decomposition.** A generic $[FeCl_5]^{2-}$ distorted structure is first compared to all the reference geometries by means of the metric $d(l, l_0)$. Once the appropriate reference orientation is chosen, the structure is decomposed into its internal and rotational contributions.

1 to a given stoichiometry and a single coordination environment. Under this approximation the problem becomes identical to the study of magneto-structral correlations, *i.e.* the fundamental approach for the individuation of new coordination environments with target properties. The individuation of magneto-structural correlations able to lead to improved magnetic properties has been the focus of the molecular magnetism for decades and here we provide a proof-of-concept that machine-learning can be exploited to provide exhaustive synthetic guidelines in a completely unbiased and automatic way, paving the way to the computational design of new magnetic molecules.

Theoretical Methods

Our machine learning strategy is based on Ridge regression and bi-spectrum components as molecular geometry fingerprints.[16–18] The first step requires the decomposition of the magnetic anisotropy over atomic contributions. It is then convenient to write $\mathbf{D}(r_i)$ over a basis of second-order spherical tensors, T^m, where m is one of the five spherical tensor components needed to describe a trace-less symmetric second-order Cartesian tensor like $\mathbf{D}$. The explicit relation between T and $\mathbf{D}$ is provided as Supplementary Information. For a molecule containing N_a atoms the decomposition reads

$$T^m = \sum_i^{N_\mathrm{a}} T^m(i) = \sum_i^{N_\mathrm{a}} \sum_j^{N_j} \alpha_j^m(i) B_j(i)\,, \tag{4}$$

where the index j runs over the N_j bi-spectrum components, B_j, describing the atomic environment of the i-th atom, and α_j^m are the coefficients that need to be determined through Ridge regression.

Magnetic anisotropy is a tensor quantity, so that Eq. (4) needs to be recast in a covariant form to ensure that the correct rotational symmetries are enforced.[19,20] Since the B terms are rotationally invariant, this is achieved by requiring the coefficients α_j to transform as

spherical tensors with respect to a reference frame rotation,

$$\alpha_j^m(i) = \sum_{m'} W_{m'}^m(l, l_0)\alpha_j^{m'}(i_0) \,, \tag{5}$$

where $W_{m'}^m(l, l_0)$ is the Wigner matrix corresponding to a rigid rotation of the atomic environment, defined by a distance cutoff, of the l-th atom with respect to the atomic environment state l_0 of the same atom chosen as reference orientation. The atom l, which defines the local environment used to perform the rotation, is chosen on the basis of the property to model. In the case of the magnetic anisotropy it is the magnetic element. Once the Ridge regression has determined the unknown coefficients $\alpha_j^{m'}(i_0)$, equations (4) and (5) can be used to predict the magnetic anisotropy for a new configuration, where its intra-molecular geometry is described by the bi-spectrum components, B_j, and its orientation in space by a Wigner matrix, $W_{m'}^m$.

The generation of the rotation matrix $W_{m'}^m(l, l_0)$ needs some careful consideration. $W_{m'}^m(l, l_0)$ is only well defined between structures with equivalent number of atoms and chemical species. When dealing with a training set containing molecules with different chemistries, a set of reference orientations l_0 is needed. For each distinct molecular configuration, it is possible to automatically select one reference orientation by introducing a distance function $d(l, l_0) = \sum_j^{N_j} |B_j(l) - B_j(l_0)|^2$ that points the reference atom l to the optimal reference state, *i.e.* the optimal reference configuration l_0 is represented by the one that minimizes $d(l, l_0)$. Once the correspondence between a molecular configuration and a reference environment is established, the rotation between the two can be computed by applying the Eckart-Sayvets conditions to the Cartesian displacements of the two set of coordinates.[21] The choice of a local reference atomic environment, instead of the entire molecular structure, is fundamental in order to maintain the local nature of the properties learned by the model.

To summarize, the procedure that lead to the calculation of a local property of atom l through Eq. (5) involves the following steps: i) comparison of the local atomic environment of atom

l with the selected reference local atomic environments l_0, ii) calculation of the amount of rotation between the local atomic enviornment and the reference local atomic environments that minimizes $d(l, l_0)$, iii) calculation of $W^m_{m'}$, iv) calculation of the bi-spectrum components of all the atoms in the local environment of the atom l and v) calculation of Eq. (5). A schematic representation of the orientation selection process, followed by the rotational and intra-molecular structural decomposition, is provided in Fig. 1.

Results and Discussion

In order to illustrate our approach we apply it to two typical coordination environments: bi-pyramidal $[FeCl_5]^{2-}$ and trigonal prismatic $[FeCl_6]^{3-}$. For each molecule we prepare 700+700 configurations, where all the Cartesian coordinates of all the atoms are displaced by a random value within the limits ± 0.1 Å and ± 0.2 Å. The size of the maximum displacements is chosen to be large enough to guarantee a broad sampling of out-of-equilibrium configurations, while maintaining a sensible chemical structure. These random displacements are applied to the DFT-optimized geometry. We use CASSCF(5,5) to compute the magnetic anisotropy for each of these 1,400 configurations. A total of 400 prototypes are excluded from the training set and left for validation and testing purpose. Details on the ab initio calculations are provided as Supplementary Information. In this case the creation of a set of reference configurations l_0 trivially corresponds to selecting a reference atomic environment per molecule. In particular, the Fe atomic environments of the $FeCl_5$ and $FeCl_6$ optimized geometries are chosen as the reference atomic environments appearing in Eq. (5).

In order to illustrate the importance of imposing the covariance property to the Ridge regression we perform the training of a model with and without its enforcement. For this purpose the configurations in the training and test sets were rotated along the y direction by a random angle in the range $[-45° : 45°]$. Results are reported in Fig. 2 and demonstrate the improvement of the covariant method over the non-covariant one. Fig. 2 also demonstrates

the high learning rate of the model that has already achieved a converged root mean square error (RMSE) of $\sim$ 0.01 cm^{-1} in about 100 configurations/molecule. In comparison, the magnetic anisotropy for $[FeCl_5]^{-2}$ and $[FeCl_6]^{-3}$ ranges between 0.05 and 0.3 cm^{-1}.

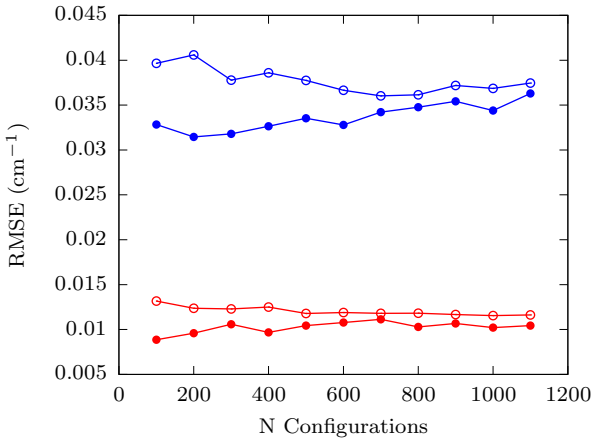

Figure 2: **Magnetic anisotropy training curve for $[FeCl_5]^{2-}$ and $[FeCl_6]^{3-}$ complexes.** The RMSE between the CASSCF anisotropy and the one predicted by machine learning for the $[FeCl_5]^{2-}$ and $[FeCl_6]^{3-}$ complexes is plotted as function of the number of configurations included in the training set. The case where covariance is enforced is displayed by red curves and symbols, while the case where covariance is not enforced is in blue. Full symbols are used for the RMSE of the training set and empty symbols for the test set.

Next we want to demonstrate that our strategy works for real systems and that can be effectively used to explore the magnetic-anisotropy landscape. To this end we show results for one of the top-performance high-anisotropy single-ion magnet $[Co(pdms)_2]^{2-}$, where pdms=1,2-bis(methanesulfonamido)benzene.[22] As shown in the inset of the bottom panel of Fig. 3, the Co^{2+} ion is tetrahedrally coordinated by RN^- ligands. We optimize the structure in vacuum and use it to generate 500 configurations with maximum displacements of $\pm$0.05 Å, 500 configurations with maximum displacement of $\pm$0.1 Å and 500 configurations with maximum displacement of $\pm$0.2 Å. We then retaine 600 of them for validation and testing purposes. For each configuration we use DFT and CASSCF to compute energy and magnetic anisotropy, respectively. More details on the construction of the bispectrum components and the regression are provided as Supplementary Information. Figure 3 shows the regression results for both axial anisotropy D and conformational energy. The test sets'

RMSE measure 1.6 kcal/mol and 2.2 cm^{-1}, respectively. Additional 131 configurations have been self-consistently sampled by molecular dynamics in the range 100 K - 400 K to enforce structural stability, as discussed previously.[18] After the inclusion of these configurations the training set's RMSE increases from 1.00 to 3.3 kcal/mol.

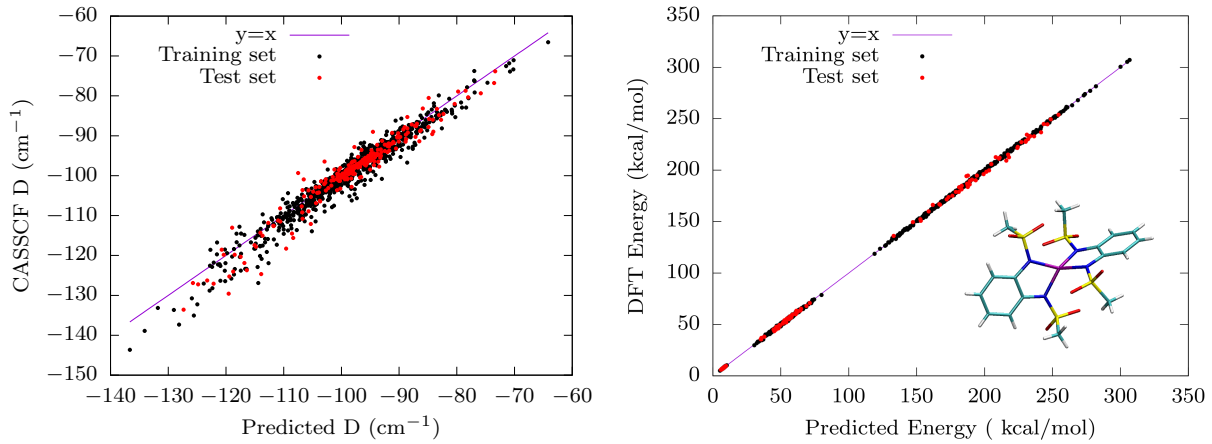

Figure 3: **Magnetic anisotropy and conformational energy training curves for $[Co(pdms)_2]^{2-}$.** The top panel shows the comparison between reference and predicted values of the axial anisotropy D, while the bottom panel reports the results for the conformational energy. Black dots corresponds to the training set and the red dot corresponds to the test one. The inset shows the molecular structure of $[Co(pdms)_2]^{2-}$, where the Co atom is coloured in Purple, Carbon atoms in Green, Hydrogen atoms in White, Sulphur atoms in Yellow, Nitrogen atoms in Blue and Oxygen atoms in Red.

The ability to reconstruct continuous structure-energy and structure-magnetic anisotropy maps with virtually no computational effort opens now the possibility to select new molecular conformations with optimal properties. We implement a particle-swarm optimization (PSO) algorithm[23] and perform a global optimization of the function in Eq. (1), specialized to the specific case,

$$\chi(r_i) = E(r_i) + \gamma D(r_i)\,. \tag{6}$$

Here the energy of a molecular conformation $E(r_i)$ and the magnetic axial anisotropy $D(r_i)$ are the features of interest. Large values of the parameter γ would allow for more severe distortions of the equilibrium molecular geometry in favour of a more favourable anisotropy. Even though magnetic anisotropy is the relevant figure of merit, the inclusion of energy

in the target quantity of Eq. (6), as suggested by Eq.(3), is of fundamental importance as it imposes the exploration of only those low-energy molecular distortions that are strongly coupled with $D(r_i)$ and excludes the sampling of totally unrealistic molecular conformations.

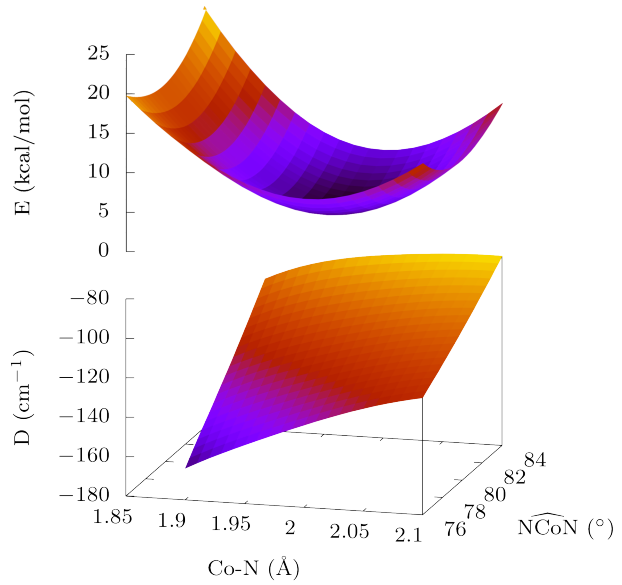

Figure 4: **2D scan of the $[Co(pdms)_2]^{2-}$ magnetic anisotropy and energy.** The axial magnetic anisotropy and the conformational energy, reported in cm^{-1} and kcal/mol respectively, are scanned along the Co-N and $\widehat{NCoN}$ directions.

The optimization of Eq.(6) shows that the magnetic anisotropy is strongly enhanced by the reduction of Co-N distances and the $\widehat{NCoN}$ angles belonging to the same pdms ligand. Running the PSO for different values of γ always lead to the same simple structural distortion. It is important to remark that the the ML model and the PSO exploration are extended to all the molecular degrees of freedom, making it possible to conclude that the magneto-structural correlation we found is the only relevant one for this specific chemical environment. The only restriction to the method is imposed by the ability of ML to make accurate predictions for geometries not included in the training set. This issue can be easily contained by implementing an active-learning scheme like the one we used to generate part of the training set with molecular dynamics.[18] In terms of efficiency it is worth remarking that the PSO optimization requires the evaluation of the function χ at least 1000 times.

This means that a comprehensive exploration of the conformational space such as the one presented here is not compatible with a brute-force use of electronic structure methods.

Fig. 4 shows the 2-dimensional scan of the molecular anisotropy and energy along a 21x21 homogeneous grid of Co-N distances and the $\widehat{\text{NCoN}}$ angles. An additional CASSCF calculation of the molecular anisotropy for the geometry corresponding to the largest absolute value of D explored in Fig. 4 confirms a good extrapolating accuracy of the ML outside the original training set with an error of $\sim 7\%$. A large spin-phonon coupling is observed for the individuated molecular motions, where a 5% reduction of the structural parameters leads to a 50% increase in the molecular anisotropy. The unexpected simplicity of this magneto-structural correlation is particularly favourable as it suggests a simple rule of thumb to chemically engineer new Co^{2+} single ion magnets with tetrahedral coordination. Our results are in perfect agreement with recent literature that reports the $\widehat{\text{NCoN}}$ angles as one of the main handle for improving Co^{+2} single ion magnets.[22,24–27] It is fundamental to remark that this result has been achieved without any bias coming from experimental studies and in a complete automatic fashion. In contrast, the experimental derivation of similar magneto-structural correlations generally take significant efforts and a cohort of different experimental characterization techniques.[22,26] Moreover, while here we are scanning the entire conformational space, experiments usually explore no more than a couple of degrees of freedom at the time. In this respect, it is not surprising that the Co-N distance magneto-structural correlation has never been reported before as little or no control is applicable to this geometrical parameter at the synthetic level.

Figure 4 also shines new light on the nature of the spin-phonon coupling in highly anisotropic compounds. The curvature of the plots corresponds to the anharmonic terms of the potential energy surface and to the spin-phonon coupling coefficients beyond the first-order. All these features are related to multi-phonons contributions to spin relaxation and their determination is expected to be crucial for the rationalization of spin dynamics in molecular compounds.[13] The computational cost of an accurate numerical estimation of second-order spin-coupling

coefficients and anharmonic couplings rapidly diverges and exceeds the cost of generating the ML model. This calculation has never been attempted before because of its computational demand and it is only possible within an accelerated framework like the one proposed here.

Conclusions

In conclusion, the method presented here can be generally applied to explore the conformational space of compounds in the search for their optimal properties, either scalar or tensorial. The complete generality of the formalism allows for readily applications in the field of molecular magnetism, where the coupling between magnetic properties and atomic motion can be parametrized and used to accelerate the individuation of magneto-structural correlations and the calculation of spin-phonon coupling coefficients. We also anticipate that this approach can be extended to the exploration of the entire chemical space, once the scheme is combined with high-throughput electronic structure theory[28] and generative models,[4] such as Variational Autoencoder[3] and Reinforcement Learning.[29]

Data and Software Availability: The training/validation/test sets and source code used to carry out the covariant Ridge regressions can be found at *https://github.com/lunghiale/fittens*.

Supplementay Information: Details on first-principles calculations, machine learning methodology and particle swarming optimization are available.

The authors declare no competing interests. This work has been sponsored by Science Foundation Ireland (grant 14/IA/2624). Computational resources were provided by the Trinity Centre for High Performance Computing (TCHPC) and the Irish Centre for High-End Computing (ICHEC). We also acknowledge the MOLSPIN COST action CA15128.

References

(1) Alberto Franceschetti and Alex Zunger. The inverse band-structure problem of finding an atomic configuration with given electronic properties. *Nature*, 402(November):60–63, 1999.

(2) Rampi Ramprasad, Rohit Batra, Ghanshyam Pilania, Arun Mannodi-kanakkithodi, and Chiho Kim. Machine learning in materials informatics : recent applications and prospects. *npj Comput. Mater.*, 3:54, 2017.

(3) Rafael Gomez-Bombarelli, Jennifer N Wei, David Duvenaud, José Miguel Hernandez-Libato, Benjamin Sanchez-Lengeling, Dennis Sheberla, Jorge Aguilera-Iparraguirre, Timothy D Hirzel, Ryan P Adams, and Alan Aspuru-Guzik. Automatic Chemical Design Using a Data-Driven Continuous Representation of Molecules. *ACS Cent. Sci.*, 4:268–276, 2018.

(4) Benjamin Sanchez-Lengeling and Alan Aspuru-Guzik. Inverse molecular design using machine learning: Generative models for matter engineering. *Science*, 361:360–365, 2018.

(5) Keith T. Butler, Daniel W. Davies, Hugh Cartwright, Olexandr Isayev, and Aron Walsh. Machine learning for molecular and materials science. *Nature*, 559:547–555, 2018.

(6) By Mark H Kryder, Edward C Gage, Terry W McDaniel, William A Challener, Robert E Rottmayer, Ganping Ju, Yiao-Tee Hsia, and M Fatih Erden. Heat Assisted Magnetic Recording. *Proc. IEEE*, 96(11):1810–1835, 2008.

(7) B Y Mueller, T Roth, M Cinchetti, M Aeschlimann, and B Rethfeld. Driving force of ultrafast magnetization dynamics. *New J. Phys.*, 13:123010, 2011.

(8) J C Slonczewski. Anisotropy and Magnetostriction in Magnetic Oxides. *J. Appl. Phys.*, 32:S253, 1961.

(9) Sebastian F Maehrlein, Ilie Radu, Pablo Maldonado, Alexander Paarmann, Michael Gensch, Alexandra M Kalashnikova, Roman V Pisarev, Martin Wolf, Peter M Oppeneer, Joseph Barker, and Tobias Kampfrath. Dissecting spin-phonon equilibration in ferrimagnetic insulators by ultrafast lattice excitation. *Sci. Adv.*, 4:eaar5164, 2018.

(10) Alessandro Lunghi, Federico Totti, Roberta Sessoli, and Stefano Sanvito. The role of anharmonic phonons in under-barrier spin relaxation of single molecule magnets. *Nat. Commun.*, 8:14620, 2017.

(11) Luis Escalera-moreno, José J Baldoví, Alejandro Gaita-Ariño, and Eugenio Coronado. Spin states , vibrations and spin relaxation in molecular nanomagnets and spin qubits : a critical perspective. *Chem. Sci.*, 9:3265–3275, 2018.

(12) Samuel J Whiteley, Gary Wolfowicz, Christopher P Anderson, Alexandre Bourassa, He Ma, Meng Ye, Gerwin Koolstra, Kevin J Satzinger, Martin V Holt, F Joseph Heremans, Andrew N Cleland, David I Schuster, Giulia Galli, and David D Awschalom. Spin–phonon interactions in silicon carbide addressed by Gaussian acoustics. *Nat. Phys.*, 15:490–495, 2019.

(13) Alessandro Lunghi and Stefano Sanvito. How do phonons relax molecular spins? *Sci. Adv.*, 5:eaax7163, 2019.

(14) R. Sessoli, D. Gatteschi, a. Caneschi, and M. a. Novak. Magnetic bistability in a metal-ion cluster. *Nature*, 365(6442):141–143, 1993.

(15) Frank Neese, Mihail Atanasov, Giovanni Bistoni, Dimitrios Manganas, and Shengfa Ye. Chemistry and Quantum Mechanics in 2019 – Give us Insight and Numbers. *J. Am. Chem. Soc.*, 141(7):2814–2824, 2019.

(16) Albert P. Bartók, Mike C. Payne, Risi Kondor, and Gábor Csányi. Gaussian approximation potentials: The accuracy of quantum mechanics, without the electrons. *Phys. Rev. Lett.*, 104:136403, 2010.

(17) Aidan P. Thompson, Laura P. Swiler, Christian R. Trott, Stephen M. Foiles, and Garritt J. Tucker. A Spectral Analysis Method for Automated Generation of Quantum-Accurate Interatomic Potentials. *J. Comput. Phys.*, 285:316–330, 2015.

(18) Alessandro Lunghi and Stefano Sanvito. A unified picture of the covalent bond within quantum-accurate force fields : From organic molecules to metallic complexes ' reactivity. *Sci. Adv.*, 5:eaaw2210, 2019.

(19) Aldo Glielmo, Peter Sollich, and Alessandro De Vita. Accurate interatomic force fields via machine learning with covariant kernels. *Phys. Rev. B*, 95:214302, 2017.

(20) Andrea Grisafi, David M. Wilkins, Gábor Csányi, and Michele Ceriotti. Symmetry-Adapted Machine Learning for Tensorial Properties of Atomistic Systems. *Phys. Rev. Lett.*, 120(3):036002, 2018.

(21) Natale Neto and Luca Bellucci. A new algorithm for rigid body molecular dynamics. *Chem. Phys.*, 328(1-3):259–268, 2006.

(22) Yvonne Rechkemmer, Frauke D Breitgoff, Margarethe Van Der Meer, Mihail Atanasov, Michael Hakl, Milan Orlita, Petr Neugebauer, Frank Neese, Biprajit Sarkar, and Joris Van Slageren. A four-coordinate cobalt(II) single-ion magnet with coercivity and a very high energy barrier. *Nat. Comm.*, 7:10467, 2016.

(23) James Kennedy and Russell Eberhart. Particle Swarm Optimization. *Proc. IEEE Int. Conf. Neural Networks*, 4:1942–1948, 1995.

(24) Majed S Fataftah, Joseph M Zadrozny, Dylan M Rogers, and Danna E Freedman. A Mononuclear Transition Metal Single-Molecule Magnet in a Nuclear Spin-Free Ligand Environment. *Inorg. Chem.*, 53:10716–10721, 2014.

(25) Elena Carl, Serhiy Demeshko, Franc Meyer, and Dietmar Stalke. Triimidosulfonates as

Acute Bite-Angle Chelates : Slow Relaxation of the Magnetization in Zero Field and Hysteresis Loop of a Co(II) Complex. *Chem. - Eur. J.*, 21:10109–10115, 2015.

(26) Elizaveta A Suturina, Joscha Nehrkorn, Joseph M Zadrozny, Junjie Liu, Mihail Atanasov, Thomas Weyhermu, Dimitrios Maganas, Stephen Hill, Alexander Schnegg, Eckhard Bill, R Long, and Frank Neese. Magneto-Structural Correlations in Pseudotetrahedral Forms of the $[Co(SPh)_4]^{2-}$ Complex Probed by Magnetometry , MCD Spectroscopy , Advanced EPR Techniques , and ab Initio Electronic Structure Calculations. *Inorg. Chem.*, 56:3102–3118, 2017.

(27) Tao Wu, Yuan-Qi Zhai, Yi-Fei Deng, Wei-Peng Chem, Tao Zhang, and Yan-Zhen Zheng. Correlated Magnetic Anisotropy to the Subtle Coordination Geometry Variation of a Series of Cobalt(II)-Sulfonamide Complexes. *Dalt. Trans.*, 48:15419–15426, 2019.

(28) Stefano Curtarolo, Gus L.W. Hart, Marco Buongiorno Nardelli, Natalio Mingo, Stefano Sanvito, and Ohad Levy. The high-throughput highway to computational materials design. *Nat. Mater.*, 12(3):191–201, 2013.

(29) Mariya Popova, Olexandr Isayev, and Alexander Tropsha. Deep reinforcement learning for de novo drug design. *Sci. Adv.*, 4:eaap7885, 2018.

Graphical TOC Entry

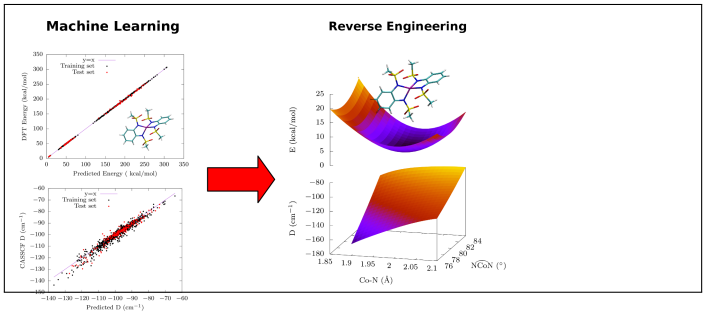

Machine learning can represent continuous structure property maps and allow to performe reverse engineering of single-ion anisotropy.

Surfing Multiple Conformation-Property Landscapes *via* Machine Learning: Designing Single-Ion Magnetic Anisotropy. Supplementary Information.

[1]Alessandro Lunghi* and [1]Stefano Sanvito
[1]*School of Physics, AMBER and CRANN Institute, Trinity College, Dublin 2, Ireland*

ANISOTROPY DECOMPOSITION IN SPHERICAL HARMONICS

The decomposition of the Cartesian tensor D_{ij} into a 2-rank spherical harmonics T^m, with $m = -2, 2$, is done accordingly to the relations

$$T^0 = \frac{1}{\sqrt{6}}(3D_{33} - (D_{11} + D_{22} + D_{33}))\,, \tag{1}$$

$$T^{-1} = \frac{1}{2}(D_{13} + D_{31} - i(D_{23} + D_{32}))\,, \tag{2}$$

$$T^{1} = -\frac{1}{2}(D_{13} + D_{31} + i(D_{23} + D_{32}))\,, \tag{3}$$

$$T^{-2} = \frac{1}{2}(D_{11} - D_{22} - i(D_{12} + D_{21}))\,, \tag{4}$$

$$T^{2} = \frac{1}{2}(D_{11} - D_{22} + i(D_{12} + D_{21}))\,. \tag{5}$$

AB INITIO CALCULATIONS

The ORCA software [1] has been employed for all the calculations. We have used the basis sets def2-TZVP for C, N and S species and the def2-SVP for C and H species. The def2-TZVP/C auxiliary basis set has been used for all the elements. The calculations of the **D** tensor have been carried out at the CASSCF level of theory, with a (7,5) active space and spin-orbit contributions included through quasi-degenerate perturbation theory. The calculations of the conformational energy has been performed at the DFT level with the PBE functional [2].

SUPERVISED LEARNING.

The coefficients α of the machine learning model where determined by linear Ridge regression:

$$\min_{\{\alpha_j\}} \left[\|T^m_{\mathrm{QM}}(\{r_i\}) - T^m_{\mathrm{ML}}(\{r_i\},\{\alpha^m_j\})\|^2 + \lambda\|\{\alpha^m_j\}\|^2\right]\,. \tag{6}$$

where the first term corresponds to the canonical least-square-fitting of the T^m_{QM} first principles reference values, and the second one to the regularization term. The optimal value of λ was chosen as to minimise the error on the validation set. The code LAMMPS [3] has been used to generate the bi-spectrum components. In all cases the order $2J = 8$ for the bi-spectrum components, corresponding to 56 elements per atomic species, has been used. The number of atomic species is a variable that can be adapted to increase the accuracy of the model and does not necessarily need to correspond to the chemical elements. The regression of $Co(pdms)_2$'s energy was computed by increased the number of atomic species to nine by discriminating chemically-inequivalent chemical elements. Conversely, the regression of $Co(pdms)_2$'s magnetic anisotropy was carried out by only considering the atoms within the radial cutoff distance from the Co atom. In the latter case the correspondence between atomic species and chemical elements was used. The radial cutoff R_{cut} used to build the bi-spectrum components have been optimised as to minimise the overall error on the training/validation set and fixed to 3.5 Å for $Co(pdms)_2$'s magnetic anisotropy, 3.1 Å for $Co(pdms)_2$'s energy and 4.5 Å for both $FeCl_x$'s energy and magnetic anisotropy. The definition of bi-spectrum components gives the possibility to differentiate atomic kinds with weights and atomic radii[4]. In this work we have set all the weights to unity and kept all the atomic radii equal to 0.5. The latter condition corresponds to using the same R_{cut} for every species. The covariancy of Ridge regression for tensorial properties requires the estimation of the amount of rotation between each configuration and the reference molecular orientations. This was estimated by applying the Eckart-Sayvets conditions[5]. This approach provide the rotation matrix that brings the Cartesian coordinates of a structure into those of a rotated one by taking into account that a rigid translation and an intra-molecular motion might also have occurred. This rotation matrix can be interpreted in terms of Euler's angles. The latter are then used to compute the Wigner rotation matrix that appears in Eq. 5 of the main text.

PARTICLE SWARM OPTIMIZATION.

The $\alpha - th$ particle in the swarm corresponds to a vector p^α that stores the position of every atom in space. The vectors p^α are propagated by summing them with the particle velocity v_α. The velocity of each particle

* lunghia@tcd.ie

in the swarm was updated at each $i-th$ step with a simple scheme: $v_\alpha^{i+1} = \omega v_\alpha^i + \Gamma[c_1 p_{best}^\alpha + c_2 p_{best}]$. p_{best}^α corresponds to the vector p^α that scored the best in the history of the particle α, while p_{best} correspond to the vector that scored the best among all the particle in the swarm. The coefficients ω and Γ were chosen as 0.7 and 1.70, respectively. The coefficients c_1 and c_2 are random number in the range [0:1]. Tests with different values of γ and number of particles have been carried out with no significant difference in the results.

[1] Frank Neese. The ORCA program system. *Wiley Interdiscip. Rev. Comput. Mol. Sci.*, 2(1):73–78, jan 2012.

[2] John P Perdew, Kieron Burke, and Yue Wang. Generalized gradient approximation for the exchange-correlation hole of a many-electron system. *Phys. Rev. B*, 54:533–539, 1996.

[3] Steve Plimpton. Fast Parallel Algorithms for Shor-Range Molecular Dynamics. *J. Comput. Phys.*, 117:1–19, 1995.

[4] Aidan P. Thompson, Laura P. Swiler, Christian R. Trott, Stephen M. Foiles, and Garritt J. Tucker. A Spectral Analysis Method for Automated Generation of Quantum-Accurate Interatomic Potentials. *J. Comput. Phys.*, 285:316–330, 2015.

[5] Natale Neto and Luca Bellucci. A new algorithm for rigid body molecular dynamics. *Chem. Phys.*, 328(1-3):259–268, 2006.